

Recycled plastic material properties defined by nanoindentation

Zdenka Prochazkova*, Vlastimil Kralik, Jiri Nemecek, Michal Sejnoha

Department of Mechanics, Faculty of Civil Engineering, Czech Technical University in Prague, Thakurova 7, Prague 6, 16629, Czech Republic

*Corresponding author. Tel: (+420) 724513713; E-mail: zdenka.prochazkova@fsv.cvut.cz

Received: 14 September 2015, Revised: 10 November 2015 and Accepted: 05 December 2015

ABSTRACT

Introduction of recycled plastic materials in structural applications such as bridges, retaining walls or railway sleepers requires a proper identification of necessary material properties. Given similarities in the microstructure of various structural elements we limit our attention to beams having a rectangular cross-section. Owing to the manufacturing process the cross-section is represented by a porous-core (inner section) surrounded by a homogeneous material (outer section). The influence of microstructural details on material parameters is examined here with a reference to the elastic Young's modulus derived from nanoindentation measurements. To identify a gradual evolution of the stiffness of plastic material from the outer section into the core the grid indentation method based on the statistical evaluation of a large number of indentations was adopted. These tests were accompanied by standard static indentation measurements to address also the effect of temperature in the range of 20–40 °C. When dealing with these types of recycled plastics, even a 5 °C temperature variation leads to a significant change in the material stiffness. In addition, standard macroscopic material properties were measured by tensile tests of samples with and without the porous core and compared with microscopic parameters. The elastic modulus obtained from nanoindentation was found to be ~20 % higher than that provided by the tensile tests. Copyright © 2016 VBRI Press.

Keywords: Recycled plastic; thermoplastics; viscoelastic material; nanoindentation; microstructure.

Introduction

A recycled plastic material spreads from applications of garden tiles and furniture (**Fig. 2a**) to pedestrian bridges or even to heavy load bridges (**Fig. 2b**) [C.F., 1-3]. The recycled plastic of our research is made by mechanical (secondary) recycling [4, 5]. It is a mixture of thermoplastics and was provided by Lankhorst Engineered Products from the Netherlands. For mechanical recycling the plastic waste is sorted, cleaned, chopped into 5-8 mm pieces, heated and pressed into a mould of a desired shape. The plastic waste has to be of the same plastic material otherwise the particles do not blend and a resulting material is low quality [4, 6]. The sorting of plastic waste is difficult because of large varieties of plastics [7]. This is paid off not only by simple and economic manufacture but also by finding good applications, where advantages of recycled plastic are well used [8-11] to cite a few.

Recycled plastic is durable, water and insect resistant and does not need any paint. Therefore, recycled plastic replaces a timber in structures where timber is expensive in terms of maintenance [10, 12, 13]. Apart from that, using recycled plastic material in structures eliminates a large amount of plastic waste [8].

An interesting application, where recycled plastic gains attention are railway sleepers [11, 14]. In this application the advantage of simple shaping of plastic material can be effectively used and also the damping effect of a recycled plastic might be beneficial for the whole structure of a rail

[14]. For such and similar structural applications it is, therefore, crucial to acquire knowledge about the material and its mechanical properties. The recycled plastic material was thoroughly examined by compression, tensile and bending tests. The tests were conducted on small test samples (cubic or dog-bone) as well as large-scale structural beams providing some useful information about the macroscopic response.

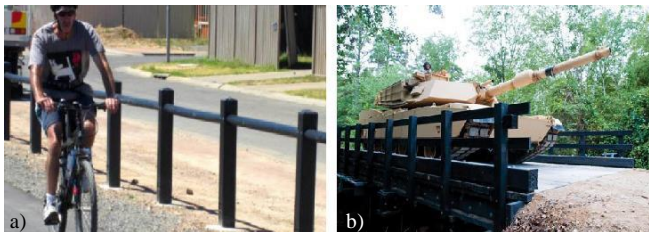


Fig. 1. a) Fencing made of recycled plastic in South Australia (1); b) completed T-8518 bridge made of recycled plastic at Fort Bragg, NC (Source: U.S. Army) ; c) cut of a standard recycled plastic beam [16].

For the modelling purposes the material response on a smaller scale plays an important role as the mechanical properties depend on the position within the beam cross-section. This is directly linked to the manufacturing process requiring the introduction of a foaming agent into the mixture [15] to arrive at specimens with more or less straight edges. More details related to the manufacturing process are provided in section -results and discussion. As a

result of this process we identify two distinct regions visible in **Fig. 1c**, a porous core surrounded by a homogeneous shell. To examine the influence of the production process on mechanical properties is the principal objective of this contribution. The present contribution is purely experimental, see section - experimental, with particular attention devoted to nanoindentation. Supplementary results provided standard tensile tests are also provided. The acquired results are summarized in section - experimental. Exploitation of these results in analytical homogenization is presented in [16] where microstructural details of the core are studied more thoroughly.

Experimental

We begin in section- tensile test with an experimental investigation based on standard tensile tests to show the rate dependent behaviour of the studied material as well as the influence of the porous core on macroscopic behaviour. This is followed by nanoindentation tests in section – nanoindentation to examine both the influence of the location of a material point within the beam cross-section and the influence of the temperature on associated mechanical properties.

Tensile test

Two types of tensile bars were tested – small ISO bars and large bars. The cross-section of ISO bars was $4 \times 10 \text{ mm}^2$ in area and their effective length was 85 mm. The loading program assumed a testing speed of 1, 5, 10, 50 and 100 mm/minute. The large bars for tensile tests were manufactured using the same recycled plastic material as ISO bars containing, unlike the small samples, also the porous core. The cross-section of large tensile samples was $15 \times 30 \text{ mm}^2$ in area and their effective length was 150 mm. The large samples were tested with a 50 mm/minutes testing speed only. The resulting loading curves are presented in **Fig. 2**.

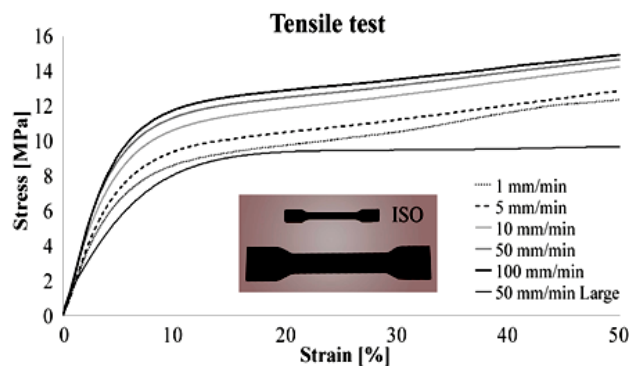


Fig. 2. ISO tensile test sample and a large sample (Large) with a porous core subjected to variable testing rates.

Clearly, the effect of porous core on the mechanical response is significant. These results also suggest a strong rate and time dependency of the studied material. The basic material properties extracted from the tensile tests, also confirming the rate dependent response of the recycled plastic material under investigation, are listed in **Table 1**. For illustration, the homogenized results derived from a

large porous sample are presented in the last row of **Table 1**.

Table 1. Young's modulus, yield stress and hardening modulus from tensile tests.

Tensile test				
v [mm/min]	E [MPa]	H [MPa]	σ_y [MPa]	$\bar{\sigma}_y$ [MPa]
1	177	9.1	4.9	8.4
5	182	8.3	5.6	9.4
10	242	7.7	6.0	10.9
50	247	7.1	6.2	11.4
100	259	7.0	7.6	11.8
Tensile test – large sample (with porous core)				
v [mm/min]	E [MPa]	H [MPa]	σ_y [MPa]	$\bar{\sigma}_y$ [MPa]
50	147	2.3	3.6	9

A graphical representation of the measured data and their extraction from the loading diagrams is evident in **Fig. 3**. While standard way of determining the yield stress σ_y as a stress associated with the intersection of the loading curve with a line (dashed line in **Fig. 3**) drawn parallel to the elastic part of this curve at the offset of 0.2 % of permanent strain, the yield stress $\bar{\sigma}_y$ was found in accord with the simplified stress-strain law to be used in numerical analyses, see the sketch in **Fig. 3**, as the intersection of two tangents to the actual loading curve one representing the initial Young's modulus E and the other defining the hardening modulus H .

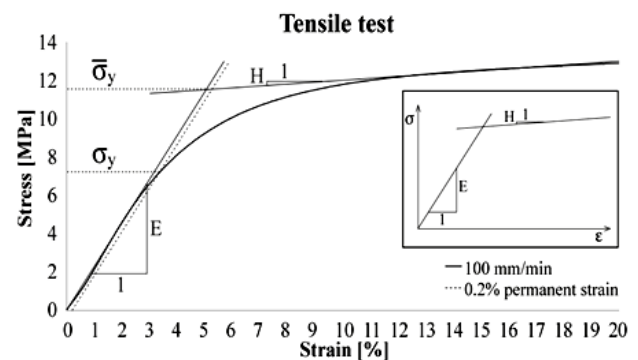


Fig. 3. Example of the stress-strain curve to identify the definition of individual material parameters in **Table 1**.

Nanoindentation

The indentation measurements were performed using the Hysitron TriboIndenter® SPM imaging with active antivibration stage nanoDMA, a transducer SN5-465-74 and the Berkovich tip, see **Fig. 4a**. The device was capable of the maximum load of 9.5 mN.

The tested specimen was cut from a large tensile test sample in **Fig. 2** having a porous core seen also in **Fig. 5b** and **Fig. 6**. This porosity is caused by the manufacturing procedure mentioned already in the introductory part and described in more detail in section – results and discussion. The sample was 15 mm wide and 20 mm long. Before

testing, the specimen was soaked with the epoxy resin and after curing the tested surface was carefully polished.

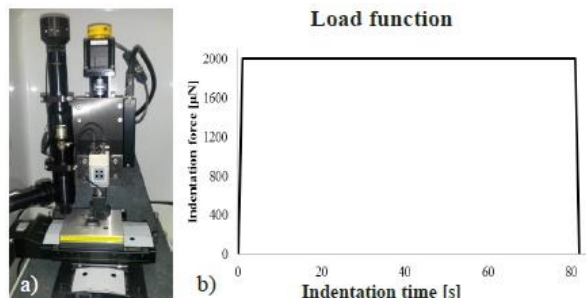


Fig. 4. a) Hysitron TriboIndenter® in-situ; b) Step load function – the sample was loaded up to 2000 µN within first second, held for 80 seconds, and then unloaded within 1 second.

Point out that the measurements were carried out with no temperature control since expecting no particular effect of small temperature fluctuations during the day time – morning vs. evening, or the temperature changes during the day and night. Nevertheless, even small temperature changes recorded in the course of measurements provided interesting results. However, we noticed that even a small temperature increase of about 5 °C resulted in a significant decrease of the measured indentation (reduced) modulus, see Table 2. This phenomenon is typical of thermoplastics [17] and will be studied in more details subsequently.

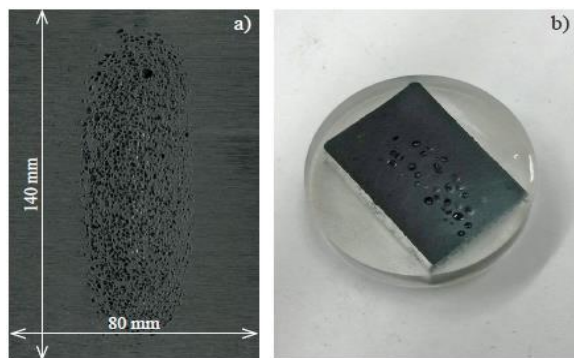


Fig. 5. a) Cut of a standard recycled plastic beam [16]; b) polished test sample of recycled plastic material with a porous core poured into an epoxy resin.

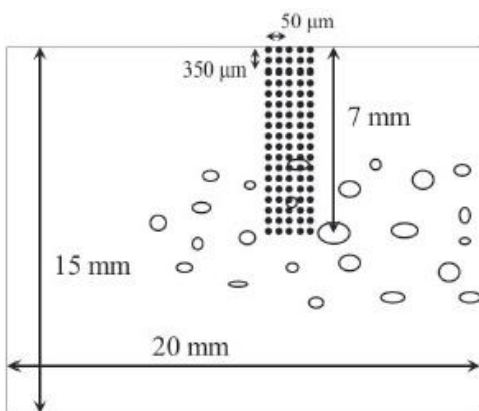


Fig. 6. Sketch of a tested sample with a depicted indentation grid.

The specimen was indented in a 5 × 20 grid displayed in Fig. 6 moving from the specimen edge towards the porous core. Evolution of the measured reduced modulus is presented in Fig. 7, where level 0 corresponds to indents in the proximity of the core centre, see the innermost row of indented points in Fig. 6, and level 20 corresponds to indents close to the edge of the specimen, the last outer row of indented points. Clearly, the reduced modulus decreases towards the edge of the product.

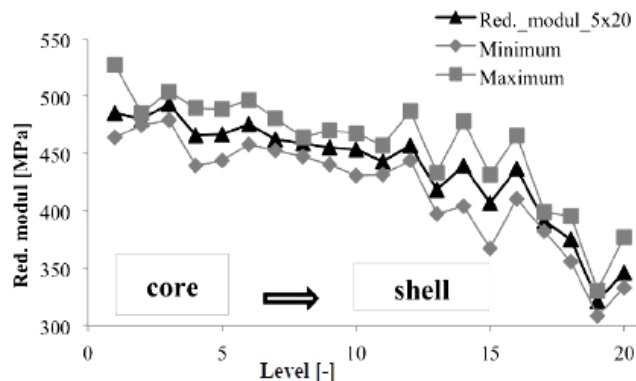


Fig. 7. Reduced modulus with respect to the position within the test sample. The plotted value of the reduced modulus is an average value of five indents at a given row of the grid.

Table 2. Parameters found by nanoindentation for the porous core and the surrounding homogeneous shell for three different temperatures.

Position	Temperature	Contact Depth	Standard Deviation	Reduced Modulus E_r	Standard Deviation	Young's Modulus E	Hardness H	Standard Deviation
	°C	[nm]						
Core	23	1909	89	495	33	416	20.5	2
	30	1922	71	385	17	324	20.2	1
	35	2047	108	356	24	300	17.9	2
Shell	23	2198	89	336	28	282	15.6	1
	30	2150	91	277	23	233	16.3	1
	35	2337	88	269	20	226	13.8	1

Such a detailed variation of the reduced modulus would become unnecessarily difficult to adopt on a large scale numerical simulations including homogenization analysis at the level of the porous core [16] where the knowledge of an average response inside the core and in the surrounding shell should be sufficient. To that end, a new set of measurements was carried out using a 3 × 3 grid of indentation points being 50 µm. This grid was randomly placed at six locations within each region thus amounting to 54 measured values of the reduced modulus for each region. These measurements were then used to calculate the

Young modulus employing the Oliver-Pharr equation [18] derived for isotropic materials in the form,

$$\frac{1}{E_r} = \frac{(1-\nu^2)}{E} + \frac{(1-\nu_i^2)}{E_i} \quad (1)$$

where, E_r is the reduced modulus measured by nanoindentation, E and ν are Young's modulus and Poisson's ratio of a measured material and E_i and ν_i are Young's modulus and Poisson's ratio of the indenter ($E_i = 1141$ GPa and $\nu_i = 0.07$) having here a negligible effect. Averages of the measured and calculated parameters together with their standard deviations found from 54 measurements for three particular temperature values are stored in **Table 2**.

Results and discussion

Young's moduli for three different temperatures and two locations are presented in **Table 2**. Young's modulus of the material inside the porous core was found to be of about 32 % higher than that of the material outside the porous core (the surrounding homogeneous shell) for the temperature of 23 °C. For temperatures equal to 30 °C and 35 °C the differences were about 28 % and 25 %, respectively. Such a significant difference was unexpected. A partial explanation can be drawn when looking closely into the manufacturing process resulting in the porous core, which hardens under the low pressure compared to the shell.

In particular, the heated liquid material is pressed into a steel mould. The temperature of the melt is about 200 °C and the temperature of the mould is about 25 °C. When the melt gets into the contact with the mould it starts to harden because its temperature drops down. But to fill the mould of, e.g. 3 meters long beam takes about half an hour. Within that time the mould is heated by the melt and the temperature difference is not that large. When the mould is almost filled the injection machine maintains high pressure (pressure of machine can be from 5 to 10 MPa depending on the machine type). Then the mould is closed and the pressure drops down and spreads over the whole melt. At pressure of about 1 MPa the foaming agent in the melt starts to expand and creates pressure to keep the edges of a beam straight while it cools and shrinks. The foaming agent is active in the porous core, where there is still the highest temperature within the beam while cooling. By the practice it was assumed that the pressure is the most important to ensure a better quality of the material. Nevertheless, the resulting Young's modulus inside the porous core suggests that lower pressure but higher temperature for a longer time might have a significant effect on the stiffness of the recycled plastic. The indentation in a grid also shows a gradient of the reduced modulus of the material from inside the porous core towards the edge of the specimen as displayed in **Fig. 7**.

Further, when comparing the elastic moduli found from tensile tests with the results provided by nanoindentation, we have to question the reasons for a large difference. The tensile test was performed under the temperature of 18 °C. For a slow loading rate the modulus was equal to about 180 MPa, recall the first two rows in **Table 1**. To link these

results to nanoindentation measurements we may consider the results acquired from tests on shell material at 23 °C temperature rendering the modulus equal to 282 MPa, see **Table 2**. Realizing the observed trend of the Young's modulus evolution with a temperature we might expect even larger difference in the results provided by the two types of experiments. This clearly opens the question of the effect of manufacturing procedure on the resulting material properties. Remember that no foaming agent was used when producing very thin ISO bar samples for tensile tests. To reconcile these differences a set of nanoindentation measurements are currently being carried out on samples with no influence of the foaming agent for various thicknesses of the tested samples.

Conclusion

Nanoindentation testing method is a promising tool for defining properties of the final product made from recycled plastics in applications where the manufacturing procedure plays a significant role such as this case of recycled plastic beams. Here, the process of mechanical recycling and manufacturing of a usable product requires thick walls, which are affected by the addition of foaming agent for production to be successful. The addition of foaming agent creates two distinct regions within the recycled plastic beam which precludes testing these regions separately at a macroscopic level. However, employing nanoindentation it is possible to define material properties also inside the recycled plastic product. Next to these small scale measurements the macroscopic tensile tests reveal the need for accounting for the rate and temperature dependent behaviour of the recycled plastic material. A suitable method appears in using the generalized Leonov nonlinear visco-elastic material model applied successfully in a number of different applications such as polymer matrix composites or asphalt mixtures [19, 20]. Owing to a relatively complex microstructure of the porous core, elements of both analytical and numerical homogenization will be needed to reliably describe the macroscopic response of, e.g. the bridge in **Fig. 1**. This however goes beyond the present scope. Some preliminary studies can be found in [16].

Acknowledgements

This research was made with the continuous support of Lankhorst Engineered Products and the research project No. SGS15/031/OHK1/1T/11

Reference

1. Bajracharya, M.; Manolo, A. C.; Karunasena, W.; Lau, K. T.; *Mater. Des.*, **2014**, 62, 98.
DOI: [10.1016/j.matdes.2014.04.081](https://doi.org/10.1016/j.matdes.2014.04.081)
2. Chong, W. K. O.; Hermreck, C.; World's First Recycled Plastic Bridges, In ICSDC 2011: Integrating Sustainability Practices in the Construction Industry; ASCE; USA, **2011**, pp. 585 – 593.
3. Wood, K.; Tough I-beam bridge for tank traffic, *Composite Technology*, **2009**, 15, 6.
4. Al-Salem, S. M.; Lettieri, P.; Baeyens, J.; *Prog. Energy Combust. Sci.*, **2010**, 36, 103.
DOI: [10.1016/j.peccs.2009.09.001](https://doi.org/10.1016/j.peccs.2009.09.001)
5. Mastellone, M.; Thermal treatments of plastic wastes by means of fluidized bed reactors; Second University of Naples: Italy, **1999**.
6. Al-Salem, S. M.; Lettieri, P.; Baeyens, J.; *Waste Management.*, **2009**, 29, 2625.
DOI: [10.1016/j.wasman.2009.06.004](https://doi.org/10.1016/j.wasman.2009.06.004)

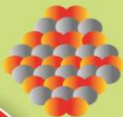
7. Hopewell, J.; Dvorak, R.; Kosior, E.; Lau, K. T.; *Philos. Trans. R. Soc. Lond. B. Biol. Sci.*, **2009**, *364*, 2115.
DOI: [10.1098/rstb.2008.0311](https://doi.org/10.1098/rstb.2008.0311)
8. Gaggino, R.; *Constr. Build. Mater.*, **2012**, *35*, 468.
DOI: [10.1016/j.conbuildmat.2012.04.125](https://doi.org/10.1016/j.conbuildmat.2012.04.125)
9. Aaron, J. F.; Finn, M. G., U. S. Patent 5807021, **1998**.
10. Trimbath, K.; Lumber made of recycled plastic prevent marine borer damage, *Civ. Eng.*, **2006**, *76*, 28.
11. Nosker, T. J.; Renfee, R. W.; Kerstein, J., Finn, M. G., U.S. Patent 6191228 B1, **2001**.
12. Nosker, T. J.; Renfee, R. W.; Recycled plastic lumber: from park benches to bridges, in *Proceedings of R'2000 5th World Congress*, **2000**.
13. Finney, D.; Recycled plastic bridge at Fort Bragg stands up tp M-1 tank traffic, *Public Works Digest*, **2009**, *12*, 7.
14. Van Belkom, A.; Analysis and comparison of sleeper parameters and the influence on track stiffness and performance, in *Railway Engineering 2015*, **2015**.
15. Semerdjiev, S.; Introduction to Structural Foam, SPE; Brookfield Center, **1982**.
16. Procházková, Z.; Králík, V.; Doubrava, K.; Šejnoha, M.; Definition of effective material properties of recycled plastic: Image analysis and homogenization, *in print "Appl. Mech. Mater."*, **2015**.
17. Van Der Vegt, A. K.; From polymers to plastics, Delft Academic Press, The Netherlands, **2006**.
18. Oliver, W. C.; Pharr, G. M.; *J. Mater. Res.*, **1992**, *7*, 1564.
DOI: [10.1557/JMR.1992.1564](https://doi.org/10.1557/JMR.1992.1564)
19. Šejnoha, M.; Zeman, J.; Valenta, R.; *Int. J. Multiscale Comput. Eng.*, **2010**, *8*, 131.
DOI: [10.1557/JMR.1992.1564](https://doi.org/10.1557/JMR.1992.1564)
20. Šejnoha, M.; Zeman, J.; *Micromechanics in Practice*, WIT Press, **2013**.

Advanced Materials Letters

Copyright © 2016 VBRI Press AB, Sweden
www.vbripress.com/aml and www.amlett.com

Publish your article in this journal

Advanced Materials Letters is an official international journal of International Association of Advanced Materials (IAAM, www.iaamonline.org) published monthly by VBRI Press AB from Sweden. The journal is intended to provide high-quality peer-review articles in the fascinating field of materials science and technology particularly in the area of structure, synthesis and processing, characterisation, advanced-state properties and applications of materials. All published articles are indexed in various databases and are available download for free. The manuscript management system is completely electronic and has fast and fair peer-review process. The journal includes review article, research article, notes, letter to editor and short communications.



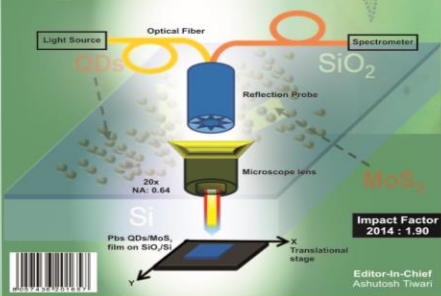
VBRI Press
a rapid publication platform

A
Monthly Journal

November 2015
ISSN 0976-3861

Advanced Materials Letters

Structure, synthesis & processing, characterization, advanced-state properties and application of materials



Editor-in-Chief
Ashutosh Tiwari

An official journal of International Association of Advanced Materials, www.iaamonline.org

Available online at
www.amlett.com and www.vbripress.com/aml